FACT complex is required for DNA demethylation at heterochromatin during reproduction in *Arabidopsis*

Jennifer M. Frost[a], M. Yvonne Kim[a], Guen Tae Park[b], Ping-Hung Hsieh[a], Miyuki Nakamura[c], Samuel J. H. Lin[a], Hyunjin Yoo[b], Jaemyung Choi[a], Yoko Ikeda[d], Tetsu Kinoshita[e,1], Yeonhee Choi[b,1], Daniel Zilberman[a,f,1], and Robert L. Fischer[a,1]

[a]Department of Plant and Microbial Biology, University of California, Berkeley, CA 94720; [b]Department of Biological Sciences, Seoul National University, 151-747 Seoul, Korea; [c]Linnean Center for Plant Biology, Department of Plant Biology, Swedish University of Agricultural Sciences, SE-75007 Uppsala, Sweden; [d]Institute of Plant Science and Resources, Okayama University, Kurashiki, 710-0046 Okayama, Japan; [e]Kihara Institute for Biological Research, Yokohama City University, Yokohama, 244-0813 Kanagawa, Japan; and [f]Department of Cell & Developmental Biology, John Innes Centre, Norwich NR4 7UH, United Kingdom

Contributed by Robert L. Fischer, April 8, 2018 (sent for review July 27, 2017; reviewed by Ryan Lister and Nathan M. Springer)

The DEMETER (DME) DNA glycosylase catalyzes genome-wide DNA demethylation and is required for endosperm genomic imprinting and embryo viability. Targets of DME-mediated DNA demethylation reside in small, euchromatic, AT-rich transposons and at the boundaries of large transposons, but how DME interacts with these diverse chromatin states is unknown. The STRUCTURE SPECIFIC RECOGNITION PROTEIN 1 (SSRP1) subunit of the chromatin remodeler FACT (facilitates chromatin transactions), was previously shown to be involved in the DME-dependent regulation of genomic imprinting in *Arabidopsis* endosperm. Therefore, to investigate the interaction between DME and chromatin, we focused on the activity of the two FACT subunits, SSRP1 and SUPPRESSOR of TY16 (SPT16), during reproduction in *Arabidopsis*. We found that FACT colocalizes with nuclear DME in vivo, and that DME has two classes of target sites, the first being euchromatic and accessible to DME, but the second, representing over half of DME targets, requiring the action of FACT for DME-mediated DNA demethylation genome-wide. Our results show that the FACT-dependent DME targets are GC-rich heterochromatin domains with high nucleosome occupancy enriched with H3K9me2 and H3K27me1. Further, we demonstrate that heterochromatin-associated linker histone H1 specifically mediates the requirement for FACT at a subset of DME-target loci. Overall, our results demonstrate that FACT is required for DME targeting by facilitating its access to heterochromatin.

FACT complex | DEMETER demethylase | chromatin | reproduction | genomic imprinting

Cytosine methylation regulates gene expression and silences transposable elements (TEs) in plants and vertebrates (1). In *Arabidopsis thaliana*, distinct DNA methyltransferases and pathways are responsible for establishing and maintaining DNA methylation in three sequence contexts: CG, CHG, and CHH, where H corresponds to A, T, or C (2). Gene body methylation is primarily CG, whereas TEs display methylation in all sequence contexts (3–5). Removal of DNA methylation occurs via the base excision repair pathway, where dual-function glycosylase/AP (apurinic/apyrimidinic) lyases catalyze excision of 5-methylcytosine from DNA and nick the sugar-phosphate backbone. Downstream, AP endonuclease, DNA polymerase, and DNA ligase function to insert cytosine in place of the excised 5-methylcytosine (6). Demethylation of TEs that overlap gene regulatory regions influences gene expression: Demethylation of transcriptional start sites and sequences that allow the binding of activating factors can promote expression, whereas demethylation of sequences that allow the binding of repressive factors can suppress gene activity.

Epigenetic reprogramming by DNA demethylation is vital for reproduction in mammals and flowering plants (7, 8). Flowering plants are the most evolutionarily successful and diverse group of plants on earth, and the defining feature of their reproduction is double fertilization. Double fertilization is mediated by multicellular male and female gametophytes, generated from haploid spores by multiple rounds of mitosis. The male gametophyte consists of two sperm cell nuclei and a vegetative cell nucleus, encased within the vegetative cell. A pollen tube germinates from the vegetative cell, delivering two sperm cells to the female gametophyte, where one fertilizes the haploid egg (which develops into the embryo) and the other fertilizes the homodiploid central cell (to form the triploid placenta-like endosperm). The embryo and endosperm, surrounded by maternal cell layers, make up the seed. The vegetative and central cells, adjacent to the sperm and egg cells, respectively, are so-called gamete companion cells. In *A. thaliana*, active DNA demethylation by the DNA glycosylase DEMETER (DME) occurs specifically in gamete companion cells, whereby highly specific transcriptional regulation during gametogenesis ensures that DME expression is confined to these cells (9–11). DME-mediated DNA demethylation occurs at thousands of discrete loci genome-wide, including the regulatory regions for genes encoding components of the polycomb repressive complex 2

Significance

The chromatin remodeling activities of the FACT (facilitates chromatin transactions) complex are required for many cellular functions, including transcription, DNA replication, and repair. Here, we demonstrate that the two FACT subunits, SSRP1 and SPT16, are also required for genome-wide DNA demethylation and regulation of gene imprinting during *Arabidopsis* reproduction. Without FACT, *Arabidopsis* seeds undergo abnormal development and exhibit aberrant DNA hypermethylation, including at imprinting control region loci. We show that FACT associates with the DEMETER (DME) DNA demethylase, facilitating DNA demethylation at over half of DME's targets, specifically those which reside in heterochromatin. These results provide insight into upstream events in the DNA demethylation pathway and reveal the importance of chromatin remodeling for DNA demethylation during *Arabidopsis* reproduction.

Author contributions: J.M.F., T.K., Y.C., D.Z., and R.L.F. designed research; J.M.F., M.Y.K., G.T.P., P.-H.H., M.N., S.J.H.L., H.Y., J.C., and Y.I. performed research; T.K., Y.C., and D.Z. contributed new reagents/analytic tools; J.M.F., M.Y.K., G.T.P., P.-H.H., M.N., S.J.H.L., J.C., Y.I., Y.C., D.Z., and R.L.F. analyzed data; and J.M.F., D.Z., and R.L.F. wrote the paper.

Reviewers: R.L., The University of Western Australia; and N.M.S., University of Minnesota.

The authors declare no conflict of interest.

Data deposition: The sequencing data reported in this paper have been deposited in the Gene Expression Omnibus (GEO) database, https://www.ncbi.nlm.nih.gov/geo (accession no. GSE105000).

[1]To whom correspondence may be addressed. Email: tkinoshi@yokohama-cu.ac.jp, yhc@snu.ac.kr, daniel.zilberman@jic.ac.uk, or rfischer@berkeley.edu.

This article contains supporting information online at www.pnas.org/lookup/suppl/doi:10.1073/pnas.1713333115/-/DCSupplemental.

Published online April 30, 2018.

(PRC2)— FERTILIZATION-INDEPENDENT SEED 2 (FIS2) and MEDEA (MEA)—inducing their monoallelic expression (i.e., genomic imprinting) in the endosperm (12). PRC2 confers H3K27me3 modifications that regulate gene expression and genomic imprinting during seed development. Activation of PRC2 component expression by DME is required for endosperm cellularization, a process essential to viable seed formation (13–15). Thus, maternal demethylation, initiated in the central cell, (9, 10) is vital for *Arabidopsis* reproduction, and loss of maternal DME results in seed abortion (9, 16–18).

Methylation removal by DME is catalyzed efficiently at CG, CHG, and CHH (9, 17). DME acts in a targeted manner and tends to demethylate relatively euchromatic TEs that are small, AT rich, nucleosome poor, and generally interspersed with genes in chromosome arms (9). DME also acts on longer, heterochromatic TEs primarily at their edges, and these TEs are prevalent in pericentromeric, gene-poor regions enriched with heterochromatic histone marks (9). How DME can successfully access regions of differing chromatin structure is not known. Chromatin structure is dictated by the organization of its functional unit, the nucleosome, consisting of an octameric core and often a linker molecule, histone H1. The core consists of two copies each of histone subunit pairs H2A/H2B and H3/H4, which can be further modified by posttranslational modifications of their NH_2-terminal amino acids (19). Chromatin structure can also be altered through changes in nucleosome presence and spacing and the exchange of canonical histone subunits for variant proteins, as catalyzed by ATP-dependent chromatin remodeling complexes and histone chaperones (19). FACT (facilitates chromatin transactions) is an essential, multidomain protein complex conserved in eukaryotes, capable of multiple interactions with nucleosome components, binding free H2A/H2B and H3/H4 dimers as well as intact nucleosomes (20, 21). FACT is required for transcription initiation and elongation; for nucleosome disassembly and reassembly, including histone variant exchange, notably of H2AX; and for chaperoning free histones (20–22). In vertebrates and plants, FACT is a heterodimer of the high-mobility group (HMG) domain STRUCTURE SPECIFIC RECOGNITION PROTEIN 1 (SSRP1) and SUPPRESSOR of TY16 (SPT16) (23–25). Further supporting the role of chromatin in DME function, the smaller FACT subunit (i.e., SSRP1) was previously shown to be involved in DME-mediated DNA demethylation at selected imprinted genes in *Arabidopsis* (26).

Here, we used *Arabidopsis* FACT complex mutants and analyzed DNA methylation genome-wide in developing seeds and in the male gametophyte to delineate how chromatin structure affects DME targeting in *Arabidopsis*. We found that DME requires the histone chaperone FACT to demethylate over half of its targets in the central cell. DME and the FACT complex protein SPT16 are located closely in the nucleus, and they interact either directly or through local intermediates. We show that chromatin structure plays an important role in determining the degree to which FACT is needed for DNA demethylation. In regions with an elevated GC ratio and high nucleosome occupancy that are enriched for heterochromatin markers such as H3K27me1 and H3K9me2, FACT is required for DME access and activity. Moreover, we demonstrate that linker histone H1 mediates the requirement for FACT at a subset of DME-target loci.

Results

FACT Is Required for DME-Mediated Genome-Wide DNA Demethylation in the Maternal Endosperm. To assess the contribution of FACT to DNA demethylation during *Arabidopsis* reproduction, we analyzed DNA methylation in plants with a nonsense mutation in the gene encoding the small, SSRP1 subunit of FACT, *ssrp1-3* (Fig. 1*A*; ref. 26). FACT is required ubiquitously in eukaryotic cells for fundamental processes, including transcriptional elongation, and seeds homozygous for complete loss-of-function mutant alleles are not viable (26–28); therefore, *ssrp1-3* mutant plants are always heterozygous.

To analyze DNA methylation in the *ssrp1-3* mutant female gametophyte, we used developing endosperm as a proxy for central cells where DNA demethylation takes place (10). Plants heterozygous for *ssrp1-3* in the Columbia-0 (Col-0) ecotype were pollinated with wild-type (WT) pollen from Landsberg erecta (L*er*) ecotype plants, and hand-microdissected F1 embryo and endosperm were isolated 8 to 10 d after pollination (DAP). The Col-0 and L*er* ecotypes differ by over 400,000 single-nucleotide polymorphisms that allow us to distinguish maternal and paternal genomes in F1 progeny (9). Whereas seeds from WT plants develop at the same rate within a given silique and rarely abort, F1 siliques from heterozygous *ssrp1-3* plants crossed to L*er* contain three groups of seeds: approximately equal numbers of normally developing viable seed and delayed viable seed (Fig. 1*B*) and rare aborting seeds with uncellularized endosperm (26). We established the frequency of the *ssrp1-3* mutant (T) and WT (C) alleles in viable seeds by subcloning and DNA sequencing genotyping amplicons. Delayed seeds had maternally inherited the *ssrp1-3* mutant allele, with a 2:1 maternal-to-paternal ratio expected for the triploid endosperm (130:63 T:C; $\chi^2 = 0.0117$, $P = 0.914$), and normal seeds had only inherited the WT allele (92 alleles counted, all C).

Next-generation bisulfite sequencing of endosperm from genotyped delayed (maternal mutant) and normally developing (WT control) seeds revealed that the *ssrp1-3* maternal endosperm genome was hypermethylated genome-wide compared with WT in the CG context (Fig. 1*C*). As controls, we used developing embryos from normal and delayed seeds as a proxy to analyze DNA methylation in the egg. Methylation of both maternal and paternal alleles in delayed embryos (*SI Appendix*, Fig. S1*A*) and the paternal endosperm genome (*SI Appendix*, Fig. S1*B*) was identical to WT, indicating that *ssrp1-3* mutant hypermethylation was inherited specifically from the maternal mutant central cell.

DME activity in the central cell promotes endosperm demethylation of maternal DNA genome-wide, and was shown previously to require SSRP1 at certain sites (9, 10, 18, 26). Alignment of WT, *ssrp1-3*, and *dme-2* endosperm methylome data (9) to the 5′ and 3′ ends of TEs and genes revealed that *ssrp1-3* hypermethylation was similar to that seen in *dme-2* maternal endosperm (9) and the paternal endosperm, which is not demethylated (Fig. 1*D* and *SI Appendix*, Fig. S1*C*). Sites of maternal hypermethylation in the *ssrp1-3* mutant endosperm genome overlap with those in *dme-2* mutant endosperm (Fig. 1*E*, black boxes; ref. 9), although regions hypermethylated only in *dme-2* mutant maternal endosperm are visible (Fig. 1*E*, green arrows). CG hypermethylated loci in *ssrp1-3* endosperm were also maternally hypermethylated at CHG and CHH contexts, (*SI Appendix*, Figs. S1 *D* and *E* and S2*A*), indicating that direct DME-mediated demethylation of CG, CHG, and CHH cytosine contexts in the *Arabidopsis* central cell is dependent on FACT. In addition, genome-wide non-CG methylation was slightly reduced globally and at TEs (*SI Appendix*, Figs. S1 *F* and *G* and S2*A*), likely due (indirectly) to DME promotion of PRC2 activity which, in turn, promotes non-CG DNA methylation (9, 29).

In the embryo, CG and CHG methylation were identical to WT (*SI Appendix*, Figs. S1*A* and S2*B*). However, we found that CHH methylation in TEs in embryo was lower in *ssrp1-3* mutants compared with WT (Fig. 1*F*). Previously, *Arabidopsis* embryos were shown to undergo a developmental increase in CHH methylation (30), and at the time of measurement, *ssrp1-3* mutant embryos were at the linear cotyledon stage compared with the bending cotyledon stage of WT sibling embryos (Fig. 1*B*). We therefore remeasured CHH methylation in WT linear cotyledon embryos and found their CHH methylation levels to be identical to the *ssrp1-3* mutant linear cotyledon embryos (Fig. 1*F*). This demonstrated that differential CHH methylation in embryos was due to developmental stage rather than the *ssrp1-3* mutation.

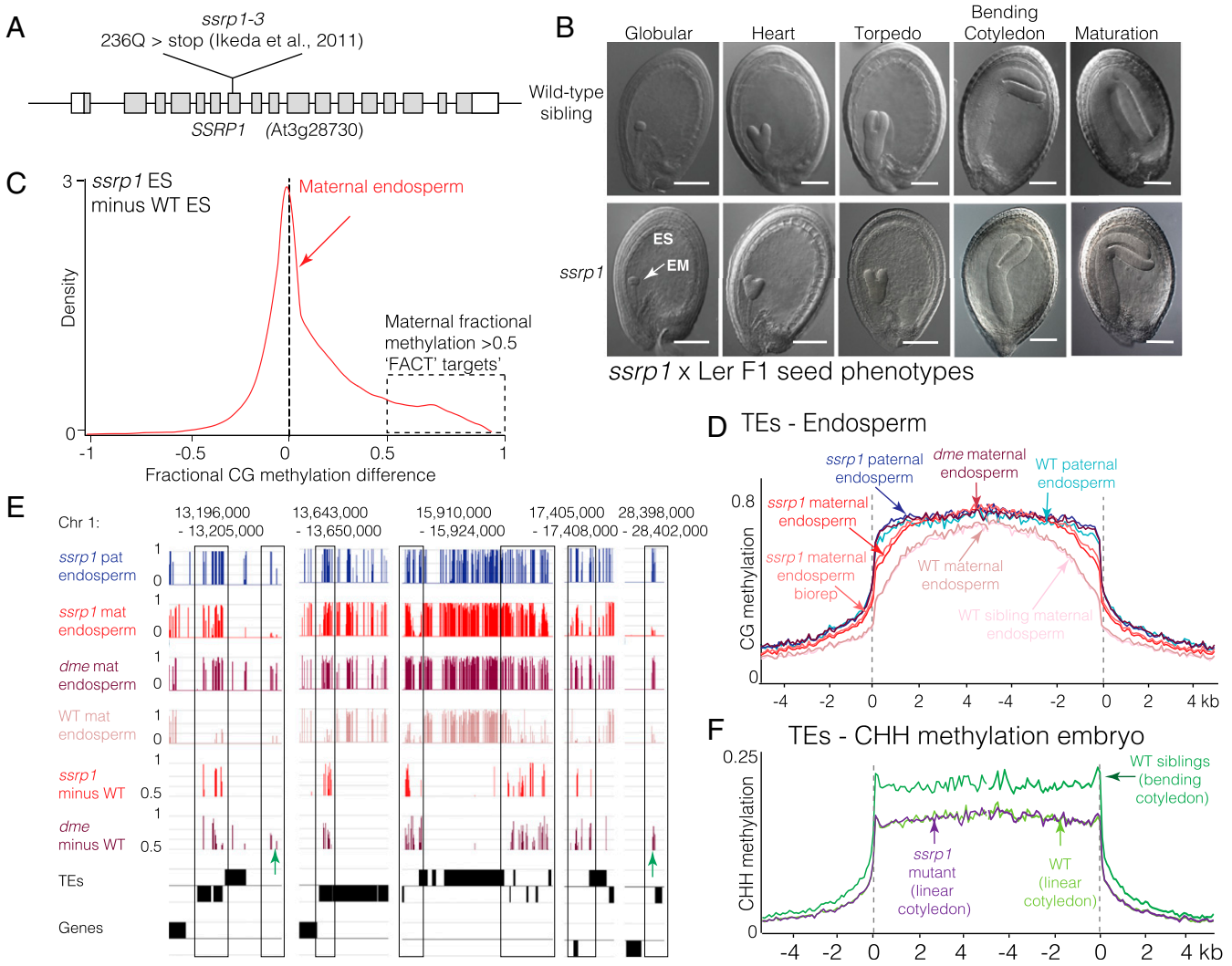

Fig. 1. FACT is required for DME-mediated genome-wide DNA demethylation in the maternal endosperm. (*A*) Diagram showing the *SSRP1* gene structure and location of the nonsense mutation *ssrp1-3* (26). (*B*) Photographs of developing F1 seeds from heterozygous *ssrp1-3* mutant plants crossed as females to WT L*er* pollen. Delayed and normal seed fractions had, respectively, inherited mutant *ssrp1-3* and WT maternal alleles. The morphological stages of WT embryos are indicated. EM, embryo; ES, endosperm. (Scale bar, 100 μm.) (*C*) Kernel density plot of CG methylation differences between *ssrp1-3* mutant endosperm (ES) and WT ES for the maternal allele. Positive numbers indicate hypermethylation, and loci whose fractional methylation level is 0.5 or greater (i.e., SSRP1/FACT targets) are indicated by the black-dotted box. (*D*) Average CG methylation in TEs in WT maternal and paternal, *ssrp1-3* mutant maternal (two biological replicates) and paternal, WT sibling maternal (from same siliques as *ssrp1-3* mutant), and *dme-2* maternal endosperm genomes. *Arabidopsis* TEs were aligned at the 5′ or 3′ end, and average methylation for all cytosines within each 50-bp interval is plotted. Dashed lines represent the points of alignment. (*E*) Genome browser alignments of DNA methylation with genes and TE annotations at selected loci of *Arabidopsis* chromosome 1. Traces show raw CG DNA methylation scores for *ssrp1-3* paternal and maternal endosperm and for *dme-2* and WT maternal endosperm (top four tracks) (9), and fractional CG methylation differences >0.5 for mutant minus WT in *ssrp1-3* and *dme-2* maternal endosperm genomes. Regions of hypermethylation that overlap in each mutant are boxed; DME-only hypermethylation is indicated by green arrows. (*F*) Average CHH methylation in WT and *ssrp1-3* mutant developing embryos, aligned according to the 5′ and 3′ ends of TEs. WT sibling and *ssrp1-3* embryos were from the same siliques at 9 DAP, but WT (linear cotyledon) embryos were dissected from siliques crossed at the same time but taken at 7 DAP, to match *ssrp1-3* embryo development (i.e., linear cotyledon) at 9 DAP.

Thus, we detected no direct effect on DNA demethylation in the *Arabidopsis* egg cell that is dependent on FACT.

FACT Is Required for Demethylation at >50% DME DMRs in Endosperm. To establish the extent to which FACT is required for DME-mediated DNA demethylation, we plotted the methylation status of *ssrp1-3* hypermethylated loci (fractional methylation difference compared with WT of >0.5 shown in Fig. 1*C*) in *dme-2* mutant endosperm (Fig. 2*A*, purple trace; ref. 9). This comparison resulted in a positive density peak (also >0.5 fractional methylation), showing that loci that become hypermethylated in *ssrp1-3* endosperm are also hypermethylated in *dme-2* mutant endosperm, and to a similar extent. A reciprocal analysis of *dme-2* hypermethylated loci in *ssrp1-3* mutant endosperm (Fig. 2*A*, red trace) has two peaks. The positive peak at >0.5 fractional methylation represents loci that are hypermethylated in both *ssrp1-3* and *dme-2* mutants—that is, they are shared DME and FACT target sites. Conversely, the peak centered on zero is indicative of sites that are only hypermethylated in *dme-2* mutant endosperm—that is, they are targets of DME, but not of FACT. By merging 50-bp windows within 300-bp regions that demonstrate a statistically significant difference in CG DNA methylation (Fisher's exact test, $P < 10^{-3}$), we created a set of FACT-mediated differentially methylated regions (DMRs). When differential methylation over the whole region was significant ($P < 10^{-10}$), we defined the region as a FACT DMR; we identified 5186 FACT DMRs of at least 100 bp

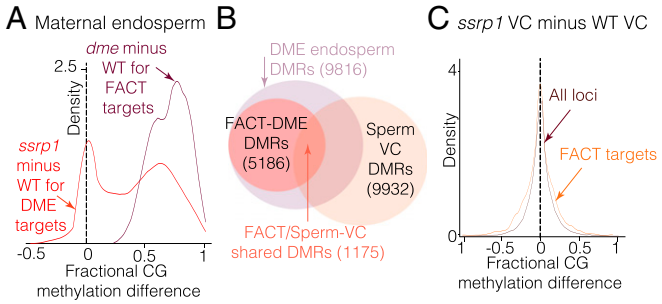

Fig. 2. FACT is required for demethylation at >50% DME DMRs in endosperm. (*A*) Red trace: kernel density plot of CG methylation differences between *ssrp1-3* and WT maternal genomes, specifically for DME targets, as defined by loci with fractional methylation >0.5 in *dme-2* mutant endosperm compared with WT. Purple trace: kernel density plot of CG methylation differences between *dme-2* and WT maternal genomes, specifically for FACT targets, as defined above. (*B*) Venn diagram depicting the overlap between significant (Fisher's exact test, $P < 10^{-10}$) DMRs of at least 100 bp in endosperm resulting from DME activity on the maternal genome (in the central cell), FACT activity on the maternal genome (FACT-DME DMRs), and DME activity in vegetative cells (Sperm VC DMRs). DME-only DMRs are those loci in endosperm which are targeted by DME, but not by FACT. (*C*) Kernel density plots of CG methylation differences between *ssrp1* vegetative cells (VC) and WT VC, showing all loci (brown trace), and FACT CG-target loci (orange trace) in maternal endosperm as defined above.

compared with 9816 DME DMRs defined previously (9) (Fig. 2*B*, *SI Appendix*, Table S1, and Dataset S1). All 5186 FACT DMRs are a subset of DME DMRs and have a slightly lower median methylation level and lower median size than DME DMRs overall (*SI Appendix*, Fig. S3). Thus, ∼53% of DME target sites in the endosperm require FACT for DNA demethylation and are referred to hereafter as FACT-DME loci; 4648 DMRs do not require FACT for efficient DNA demethylation and are referred to hereafter as DME-only loci. Thus, FACT is required for demethylation at over half the DME sites in the central cell.

We Do Not Detect a Requirement for FACT in Pollen DNA Demethylation. There are 9932 DME DMRs present between the sperm and vegetative cell genomes, and 1175 overlap with the 5186 DME DMRs in endosperm that are shared with FACT (9) (Fig. 2*B* and *SI Appendix*, Table S1). We investigated whether FACT is also required for genome demethylation in the male gametophyte by isolating sperm and vegetative cell nuclei from fluorescence-activated cell-sorted pollen harvested from *ssrp1-3* heterozygous plants. Previous work shows that the *ssrp1-3* allele has a low rate of paternal transmission to F1 seeds (26). To establish whether the *ssrp1-3* mutant allele was present at a normal level in pollen, we cloned *ssrp1-3* genotyping amplicons in our pollen sample isolated from heterozygous *ssrp1-3* plants, as we did for endosperm, finding that the paternal *ssrp1-3* and WT alleles are present in pollen at approximately equal frequency (37:44, WT:*ssrp1-3* mutant, 0.84:1; $\chi^2 = 0.3012$, $P = 0.583$). Thus, *ssrp1-3* is transmitted normally through male meiosis and subsequent mitosis so that *ssrp1-3* mutant pollen is formed. We therefore suggest that the *ssrp1-3* male transmission defect identified by Ikeda et al. (26) manifests after pollen formation. Bisulfite sequencing did not reveal hypermethylation of the mutant vegetative cell genome, either genome-wide or by specifically focusing on FACT-target loci in endosperm (Fig. 2*C*), and we did not identify any statistically significant DMRs between WT and *ssrp1-3* mutant vegetative cells. Thus, inheriting a mutant *ssrp1-3* allele does not seem to affect patterns of DME-mediated DNA demethylation in the vegetative cell.

SPT16 Contributes to DNA Demethylation and Colocalizes with DME in Nuclei. FACT consists of SSRP1 and the larger, SPT16 subunit. To establish whether SPT16 mutants exhibited similar phenotypes to *ssrp1-3*, we obtained seeds carrying a T-DNA insertion in the coding region of *SPT16*, henceforth referred to as *spt16-3* (31) (Fig. 3*A* and *SI Appendix*, Table S2). The seed phenotypes of heterozygous F1 *spt16-3* selfed or crossed to L*er* were very similar to *ssrp1-3*, with approximately the same ratios of normal and delayed seed development present (Fig. 3*B* and *SI Appendix*, Fig. S4*A* and Tables S2 and S3), and plants could not be made homozygous. Delayed seeds were highly enriched for the *spt16-3* mutant allele (*SI Appendix*, Fig. S4*B*), although seed abortion in *spt16-3* was not above background.

Plants heterozygous for *spt16-3* in the Col-0 ecotype were pollinated with WT pollen in the L*er* ecotype, and hand-microdissected F1 embryo and endosperm were isolated 8 to 10 DAP. Next-generation bisulfite sequencing was carried out to compare DNA methylation in delayed (maternal *spt16-3* mutant) versus normally developing (WT siblings) endosperm and embryos. Comparing the *spt16* mutant endosperm and embryo methylomes to WT revealed identical methylation levels in embryo and similar overall CG methylation levels in *spt16-3* mutant maternal endosperm (Fig. 3*C*, "Maternal all loci" pink trace, Fig. 3*D*, and *SI Appendix*, Fig. S4*C*). However, *spt16-3* maternal endosperm hypermethylation could be distinctly detected by kernel density analysis for only SSRP1-target loci, specifically on the maternal *spt16-3* endosperm allele (Fig. 3*C*, "Maternal for SSRP1 targets" positive purple trace and Fig. 3*E*). Moreover, by plotting the fractional methylation difference between *ssrp1-3* and WT maternal endosperm at only those loci where *spt16-3* maternal endosperm was hypermethylated (*spt16* minus WT fractional methylation >0.5 from Fig. 3*C*, defined as SPT16 targets), we show that *spt16-3* hypermethylated loci are also sites of *ssrp1-3* hypermethylation (Fig. 3*F*, purple trace). Non-*spt16-3* hypermethylated loci (fractional methylation <0.1 from Fig. 3*C*, defined as non-SPT16 targets) instead give a very different density curve (Fig. 3*F*, green trace), centered on zero and thus enriched for sites that are not hypermethylated in *ssrp1-3* endosperm. Therefore, the effect of the *spt16-3* mutation on endosperm DNA methylation is qualitatively the same as *ssrp1-3*, but weaker. These results are consistent with a model of central cell demethylation by DME mediated by both subunits of FACT.

FACT and DME Proteins Interact in the Nucleus in Vivo. To investigate the relationship between FACT and DME, we measured whether they interacted in vivo. We used the bimolecular fluorescence complementation assay (32) to detect protein–protein interactions by expressing combinations of full-length DME and the N and C termini of SSRP1 and SPT16 proteins, linked to portions of the yellow fluorescent protein (YFP) in *Arabidopsis* leaf protoplasts. We observed frequent bright fluorescent signals of reconstituted YFP in the nucleus of cells expressing SSRP1-N and SPT16-C, as expected, given that they form the FACT complex (Fig. 4 *A* and *C*; SSRP1-C and SPT16-N constructs displayed self-activity, so they were not included). We also observed bright, albeit fewer, fluorescent signals in the nucleus of cells expressing SPT16-C and DME (Fig. 4 *B* and *D*), indicating that these proteins are closely localized, possibly within the same macromolecular complex. YFP signals tended to overlap regions of intense Hoechst staining, indicating that they were localized in chromatin (Fig. 4*D*, blue staining). We observed DME and SSRP1 fluorescent signals to be very infrequent and faint (*SI Appendix*, Fig. S5*A*), indicating that the more direct interaction occurs between DME and the larger, SPT16 subunit of FACT. No reconstituted YFP signals were observed in protoplasts transfected with DME-YFP-C alone or with the control protein LHP1 (*SI Appendix*, Fig. S5 *B* and *C*). These results suggest that the FACT complex and DME are closely localized in the nucleus.

FACT Is Required to Regulate Imprinted Genes. DME-mediated demethylation in the central cell promotes both maternal and paternal expression of imprinted genes, since DNA methylation

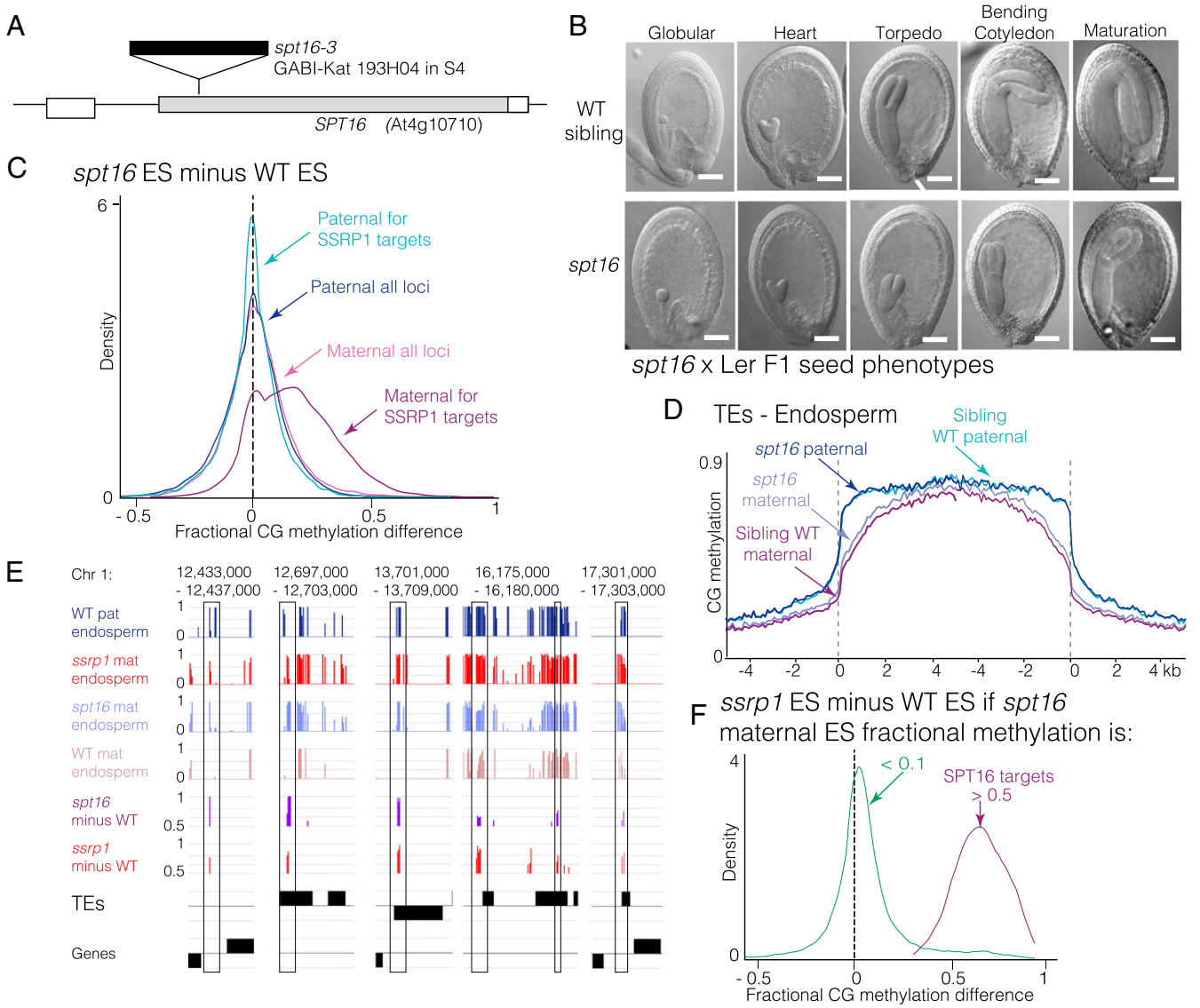

Fig. 3. SPT16 contributes to DNA demethylation. (*A*) Diagram showing the *SPT16* gene structure and location of the GABI-Kat 193H04 T-DNA insertion *spt16-3*. (*B*) Photographs of developing F1 seeds from heterozygous *spt16-3* mutant plants crossed as females to WT L*er* pollen. Delayed and normal seed fractions were used as mutant and WT control samples, respectively. The morphological stages of WT embryos are indicated. (Scale bar, 100 μm.) (*C*) Kernel density plots of CG methylation differences between *spt16-3* mutant endosperm (ES) and WT ES for maternal and paternal alleles for all sites and for SSRP1/FACT-target loci, as defined in Fig. 1C. (*D*) Patterns of TE CG DNA methylation on *spt16-3* mutant delayed maternal and paternal, and normal WT sibling (seed from same siliques) maternal and paternal endosperm alleles. *Arabidopsis* TEs were aligned at the 5′ or 3′ end, and average methylation for all cytosines within each 50-bp interval is plotted. Dashed lines represent the points of alignment. (*E*) Genome browser alignments of DNA methylation with genes and TE annotations at selected loci of *Arabidopsis* chromosome 1. Traces show raw CG DNA methylation scores for WT paternal and *ssrp1-3*, *spt16*, and WT maternal endosperm (top four tracks), and fractional CG methylation differences >0.5 for mutant minus WT maternal endosperm in *spt16-3* and *ssrp1-3*. Regions of hypermethylation overlapping in each mutant are boxed. (*F*) Kernel density plots of CG methylation differences between *ssrp1-3* mutant endosperm (ES) and WT ES, specifically for SPT16 targets, and for non-SPT16 target DNA. SPT16 CG targets are defined as those loci with a fractional CG methylation level of >0.5 in *spt16-3* mutant endosperm compared with WT, and nontargets as having a level of <0.1.

can either inhibit or promote gene transcription, depending on genomic context (33, 34). The short, euchromatic TEs over-represented in the targets of DME, and representing a large proportion of FACT-DME targets, are often found upstream of imprinted genes (9). The SSRP1 subunit of FACT was previously observed to be required for demethylation of the short interspersed nuclear element controlling imprinted FWA expression, and for expression of the PRC2 subunit MEA (26). To investigate the role of FACT in the regulation of DMRs that mediate imprinted gene expression, we surveyed maternally and paternally expressed "stringent" imprinted genes (35) and correlated them with either our genome-wide dataset of FACT target sites or with all *Arabidopsis* genes, using ends analysis (Fig. 5*A*). Similar to DME targets overall (9), FACT-DME shared target sites were significantly enriched compared with all genes (by Fisher's exact test) at the 5′ end and around the transcriptional start and termination sites of maternally expressed imprinted gene loci, indicating that the FACT-dependent subset of DME target sites do include imprinted regions (Fig. 5*A*). FACT-DME targets were also significantly enriched in the gene body of maternally expressed genes, but not at the 3′ end. FACT-DME targets were not significantly associated with paternally expressed imprinted genes. To look at individual imprinted gene loci, we analyzed DNA methylation in WT, *ssrp1-3*, *spt16-3*, and

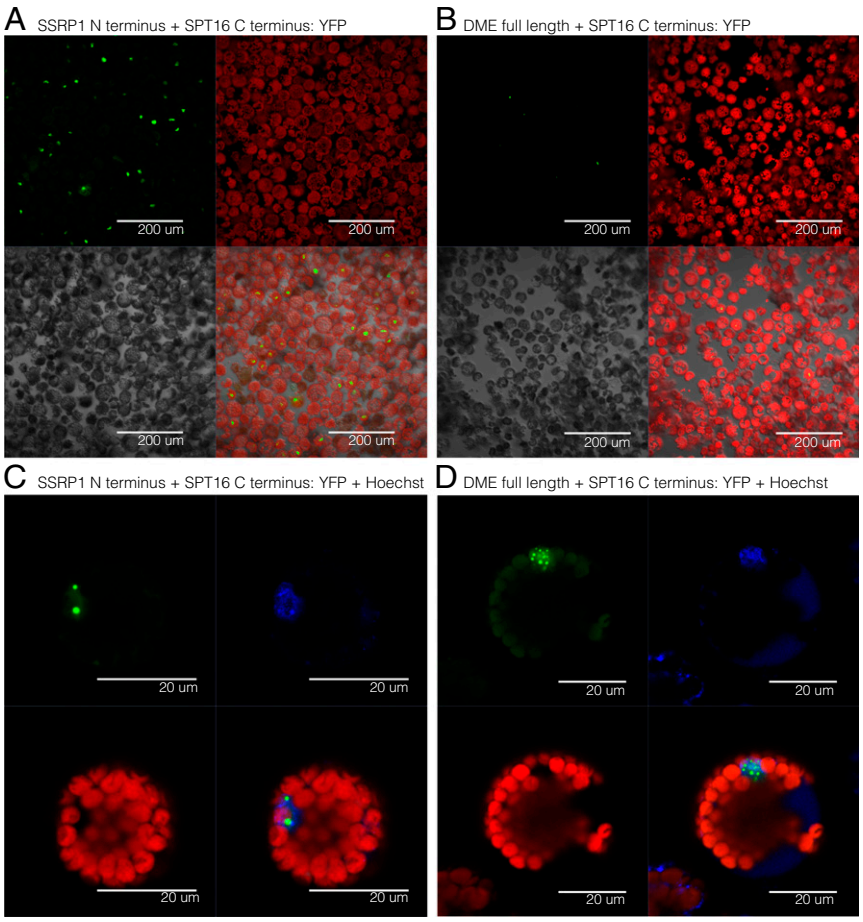

Fig. 4. FACT and DME proteins interact in the nucleus in vivo. Confocal fluorescence microscopy images from bimolecular florescence complementation assays, showing the relative frequency of interactions as represented by YFP fluorescent signals generated by interactions between SSRP1 N-terminal and SPT16 C-terminal protein domains (*A* and *C*) and between the SPT16 C-terminal domain and DME protein (*B* and *D*). *A* and *B* show lower magnification (scale bars, 200 μm) to demonstrate the frequency of interactions observed, with YFP, autofluorescence, contrast, and composite images. *C* and *D* show higher magnification (scale bars, 20 μm), with YFP, Hoechst, autofluorescence, and composite images outlining the location of fluorescent spots relative to protoplast structure, and chromatin in the nucleus stained with Hoechst 33342.

dme-2 mutant maternal endosperm for both maternally and paternally expressed imprinted genes, locus specifically (Fig. 5 *B* and *C*). Methylation of imprinting control regions for maternally expressed imprinted genes is aberrant in *ssrp1-3* and *spt16-3* endosperm (Fig. 5*B*), consistent with the contribution of FACT to imprinted gene regulation, as a function of facilitating access of DME to demethylate heterochromatic DNA. Some key imprinted genes (Fig. 5*C*) such as FIS2, which result in seed abortion when not expressed (36), do not appear to be regulated by FACT, consistent with the reduced seed abortion in *ssrp1-3* and lack of seed abortion in *spt16-3* mutant siliques compared with *dme-2* (Fig. 5*C*).

FACT Is Required for DME-Mediated Demethylation in Long TEs Enriched with H3K9me2. We next analyzed the characteristics of DME targets that require FACT for DNA demethylation. In our ends analysis of TE methylation (Fig. 1*D*), the bodies of long TEs (away from the points of alignment) exhibited similar levels of hypermethylation between *ssrp1-3* and *dme-2* mutant maternal endosperm (9). This indicates that in TE bodies, FACT is always required for DME access. However, at TE edges (close to the points of alignment), *ssrp1-3* hypermethylation was less than *dme-2* hypermethylation, indicating a decreased or variable requirement for FACT here (Fig. 1*D*). By separating TEs by size, we found that increased TE length is positively correlated with FACT-DME shared targets (Fig. 6*A* and *SI Appendix*, Fig. S6*A*), and TEs longer than ∼4 kb require FACT for DME access along their length (Fig. 6*B*). In contrast, in smaller TEs, TE edges have a variable requirement for FACT (*SI Appendix*, Fig. S6 *B* and *C*). Long TEs are enriched in pericentromeric DNA, and when we calculated the relative enrichment of FACT-DME shared and DME-only DMRs across the genome, FACT-DME shared sites were highly enriched at pericentromeric regions, whereas DME-only sites were more frequent than FACT-DME shared sites in chromosome arms (Fig. 6*C*).

DME homologs ROS1, DML2, and DML3, which act in sporophytic tissues to "prune" DNA methylation at certain sites, require histone acetyltransferase INCREASED DNA METHYLATION 1 (IDM1) and the IDM2 α-crystallin domain protein to gain access to DNA at a subset (10%) of sites in regions depleted in H3K4me2 (37, 38). To determine whether chromatin structure similarly dictates the requirement for FACT, we correlated FACT-DME and DME-only target coordinates with defined genomic regions corresponding to nine chromatin states that feature specific combinations of histone marks (39) (Fig. 6*D*). DME targets, in general, were highly enriched in heterochromatic state 8, consistent with the previously reported DME target prevalence in euchromatic TEs (9, 39). DME-only targets were comparatively more enriched than FACT-DME shared targets in euchromatic states 1 to 7, whereas FACT-DME shared sites were more frequent in the two heterochromatic states 8 and 9 (Fig. 6*D*). In particular, FACT-DME targets predominated in state 9, the GC-rich chromatin domains associated with heterochromatic TEs (Fig. 6*D*). In short TEs and TE edges, *ssrp1-3* hypermethylation is less severe than in the *dme-2* mutant (*SI Appendix*, Fig. S6 *A–C*); thus, FACT is only required for demethylation at a subset of DME short-TE targets. We correlated the groups of DME-only and FACT-DME targets with individual structural chromatin features in aerial plant tissues (40–44) in short TEs (below 1 kb). Consistent with the observations above, we found that even in short TEs, FACT is more frequently required for DME activity in GC-rich regions with high nucleosome occupancy and

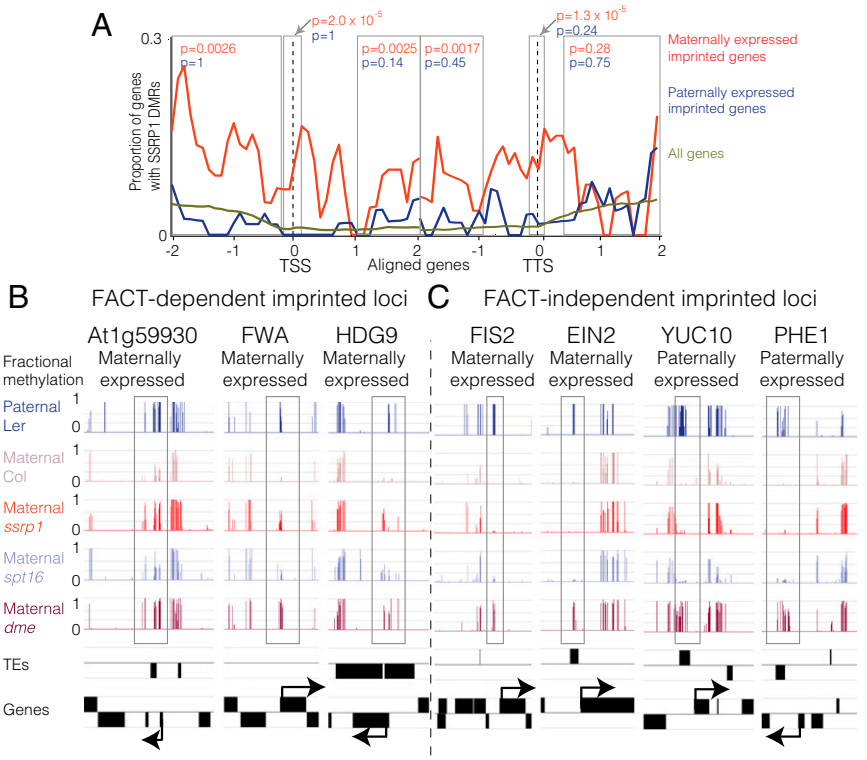

Fig. 5. FACT is required for regulation of a subset of imprinted genes. (*A*) The distribution of significantly differentially methylated regions (as in Fig. 2*B*) between *ssrp1-3* and WT maternal endosperm near to genes. Genes were aligned at the 5′ end [transcriptional start site (TSS), left dashed line] or the 3′ end [transcriptional termination site (TTS), right dashed line], and the proportion of genes with DMRs in each 100-bp interval is plotted. DMR distribution is shown with respect to maternally expressed imprinted genes (red trace), paternally expressed imprinted genes (blue trace), and all genes (brown trace). Significance of DMR enrichment with respect to all genes (Fisher's exact test) for particular genic regions is shown in gray boxes. *Arabidopsis* imprinted genes were collated from ref. 35. (*B* and *C*) Snapshots of CG methylation in endosperm near imprinted genes that were (*B*) dependent on FACT regulation (gained hypermethylation in *ssrp1-3* mutant endosperm) and (*C*) independent of FACT regulation (unaffected by *ssrp1-3* mutation). Paternal (L*er*) endosperm is shown in blue, with maternal alleles of the *ssrp1-3* mutant in red, *spt16* mutant in light blue, *dme* mutant in maroon, and maternal WT Col-0 in pink, aligned to annotated genes and TEs.

increased levels of the compact chromatin markers H3K27me1 and H3K9me2 (45) (*SI Appendix*, Fig. S6*D*). DME-only target TEs below 1 kb were comparatively enriched with markers of open chromatin (*SI Appendix*, Fig. S6*E*). In fact, by analyzing the enrichment of DME-only and FACT-DME shared targets according to TE length, the positive relationship between FACT-DME targets and increased TE length is lost only in those TEs with low H3K9me2 occupancy (*SI Appendix*, Fig. S6*F*). Thus, FACT is required for DME access to all long TEs since they tend to be heterochromatic and enriched with histone modifications such as H3K9me2. Conversely, FACT is variably required for DME access to short TEs, which are more likely to occur in open chromatin, depending on the specific chromatin structure of those TEs, and whereby at relatively euchromatic TEs, DME does not require FACT.

H1 Presence Mediates the Requirement for FACT at Certain DME-Target Loci. The SSRP1 subunit of FACT is an HMG domain protein (HMG domain proteins are known to compete with the histone linker H1 for chromatin occupancy) (46). H1 binds to the nucleosome core and is strongly associated with heterochromatin (47). In addition, its presence is known to impede DNA accessibility in both euchromatin and heterochromatin (48). H3K9me2 enrichment, which we show to often be present at loci where FACT is required for DME activity, is also correlated with regions of H1 occupancy, so we sought to determine whether H1 may impede access of DME in a manner that contributes to the requirement for FACT in DME activity.

Using plants homozygous for *h1.1* and *h1.2* alleles (49), referred to as homozygous *h1*, we generated mutant plants that were also heterozygous for *ssrp1-3*. We did not observe any rescue of the *ssrp1-3* seed delay and abortion phenotype (*SI Appendix*, Table S3), indicating that H1 does not wholly dictate the need for FACT in DME activity. To determine if H1 plays a more modest role, we pollinated plants homozygous for *h1* and heterozygous for *ssrp1-3* in the Col-0 ecotype with WT pollen in the L*er* ecotype. We then analyzed the maternal methylomes of F1 microdissected endosperm from delayed F1 seeds (maternal mutant *h1 ssrp1-3*) versus their normally developing siblings (maternal mutant *h1*), and compared them to maternal mutant *ssrp1-3* endosperm versus WT endosperm. We could not detect an obvious decrease in maternal genome-wide hypermethylation in *h1 ssrp1-3* compared with *ssrp1-3* (*SI Appendix*, Fig. S7*A*). However, by looking specifically at all DME-target loci, both genome-wide and at individual FACT-DME targets (Fig. 7 *A* and *B*, respectively), we identified a decrease in hypermethylation in *h1 ssrp1-3* compared with *ssrp1-3*, specifically at FACT-DME shared targets, consistent with an effect of H1 on FACT-DME targets, but not DME-only targets (Fig. 7 *A*–*C*). Because *h1* mutant seedling DNA is hypomethylated at euchromatic TEs genome-wide (49), it is possible that the loss of hypermethylation seen in our triple mutant was simply due to an underlying absence of DNA methylation in *h1* mutant endosperm. We analyzed *h1* mutant seedling DNA methylation specifically at loci that are differentially methylated between *h1 ssrp1* and *ssrp1* mutant maternal endosperm (Fig. 7*C*, "FACT-DME DMRs associated with H1", $n = 565$ and *SI Appendix*, Table S1). The *h1* mutant seedlings were not predominately hypomethylated at FACT-DME DMRs associated with H1 (Fig. 7*B* and *SI Appendix*, Fig. S7*B*), indicating that the lack of hypermethylation in *h1 ssrp1* mutants at FACT-DME targets is due the *h1 ssrp1* genotype rather than a hypomethylated *h1* background. The decrease in DNA methylation at FACT-DME targets in the triple mutant is only a partial return to WT levels. To investigate this partial effect, we plotted the difference between the triple-mutant and *h1* mutant siblings at FACT-DME targets. Two peaks were generated, representing two groups of sites: some that are affected by H1 and return to WT methylation levels in the triple mutant (peak on zero), and some that remain hypermethylated (Fig. 7*D*). We also plotted the fractional methylation of these sites compared with their methylation level in *ssrp1-3*, using a heat map, showing that affected and unaffected sites occur across the range of FACT demethylated sites (Fig. 7*E*). Overall, loss of H1 suppressed

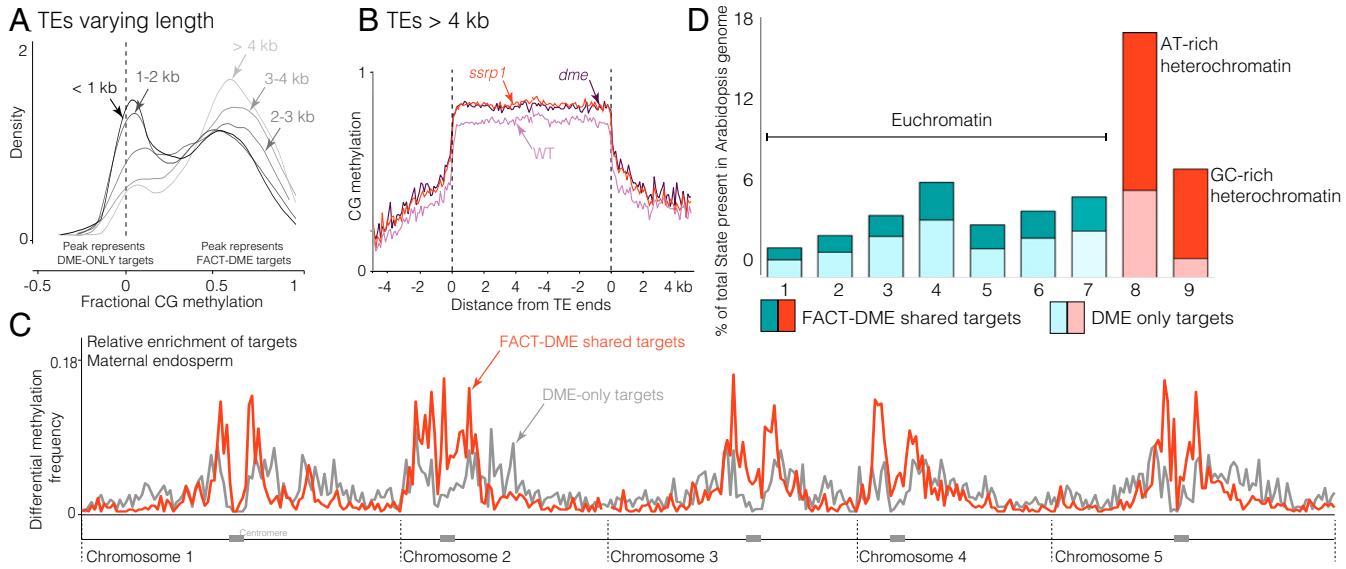

Fig. 6. FACT is required for DME-mediated demethylation in heterochromatin, but not euchromatin. (*A*) Kernel density plot of the methylation status of *dme-2* hypermethylated loci (fractional methylation difference compared with WT of >0.5) in *ssrp1-3* mutant endosperm, as in Fig. 2*A*, for loci grouped by TE length (<1 kb, 1 to 2 kb, 2 to 3 kb, and >4 kb). (*B*) Average CG methylation in TEs longer than 4 kb in WT, *ssrp1-3*, and *dme-2* maternal endosperm genomes. (*C*) Relative enrichment of FACT-DME shared and DME-only DMRs (defined as >0.5 fractional methylation difference for both, or >0.5 for DME and <0.1 for SSRP1, respectively, including at least 20 sequenced cytosines) in 300-kb intervals across the *Arabidopsis* genome. Increased density of methylation differences correlates with pericentromeric regions. (*D*) Bar chart displaying the percentage of chromatin states 1 to 9 occupied by all DME target sites; states 1 to 7 represent euchromatin (green) and states 8 to 9 represent heterochromatin (red) as defined by ref. 39. Bar detail indicates the proportion of loci occupied by DME-only (lighter shading) and FACT-DME shared (darker shading) target sites.

the hypermethylation caused by the *ssrp1-3* mutant at a subset of genomic sites, indicating that H1 may impede DME access to chromatin at these sites, which is relieved by FACT.

Discussion

Like ATP-dependent chromatin remodeling enzymes, FACT dramatically increases the accessibility of nucleosomal DNA. Current evidence suggests that FACT interaction with the nucleosome promotes formation, or stabilization, of a looser structure, still bound to DNA but more likely to undergo reorganization through H2A/H2B displacement (20, 50, 51). Our data show that FACT is required for both DME-mediated demethylation in GC-rich regions with high nucleosome occupancy and enrichment for posttranslational histone modifications associated with heterochromatic TEs, particularly H3K9me2 (Fig. 6*D* and *SI Appendix*, Fig. S6 *D* and *F*). Less than half of DME target sites are accessible without FACT involvement (Fig. 2 *A* and *B*). These DME-only sites were shorter TEs enriched with euchromatic markers such as H2Bub (Fig. 6*D* and *SI Appendix*, Fig. S6*E*) and depleted in H3K9me2, thus representing loci with chromatin that was more accessible to proteins such as DME.

Genomic loci exhibiting enrichment of H3K36me3 and H2Bub, at least in seedling tissues, were anticorrelated with sites of FACT activity in DME-mediated DNA demethylation as observed in endosperm (*SI Appendix*, Fig. S6*E*). This is striking because during transcription, H2Bub is a positive regulator of FACT (52). Similarly, methylation of H3K36 mediates the requirement for FACT in transcription initiation, and H2BK123/120Ub1 stimulates FACT activity in transcriptional elongation and nucleosome reassembly after transcription (52–54). These data indicate that the mode of FACT action with DME DNA glycosylase during reproduction differs from that during transcription. This is reminiscent of recent data from experiments in human cells showing that upon oxidative stress, FACT is relocated away from transcribed DNA to regions requiring repair, where it remodels chromatin to promote base excision repair, facilitating the interaction between 8-oxoguanine glycosylase and DNA (55).

A further key feature of heterochromatin is the association of nucleosomes with linker histone H1. FACT directly interacts with H1 in vitro and in vivo in mammalian cells (56, 57), and the SSRP1 FACT subunit has an HMG domain, which tends to compete with H1 molecules for nucleosome binding, weakening the interaction between H1 and chromatin (58). Thus, FACT may chaperone H1-containing nucleosomes in *Arabidopsis*, contributing to the enhancement of DNA accessibility for DME activity during reproduction. Removing H1 did not obviate the need for FACT in DME activity (*SI Appendix*, Fig. S7*A*); however, we found a decrease in hypermethylation specifically at FACT-DME target sites in mutant homozygous *h1* maternal *ssrp1* endosperm (Fig. 7 *A*–*C*), corresponding to ∼10% of FACT-DME target sites. This is reminiscent of chromatin-dependent mechanisms of DNA methylation (4, 49). Notably, chromatin remodeler DEFICIENT IN DNA METHYLATION 1 facilitates access of DNA methyltransferases to H1-bound chromatin (49). These data are consistent with a gradient of heterochromatic status (49) within the *Arabidopsis* central cell genome, whereby the DME targets range from euchromatic, and accessible, to more heterochromatic, where chromatin accessibility decreases below a threshold, at which point FACT is required.

The requirement for FACT in DME activity in the central cell, but not the vegetative cell, is intriguing (Fig. 2*C*). Since the vegetative cell nucleus is separated from its somatic precursor by only one cell division, it is possible that SSRP1 or SPT16 proteins are still present in this tissue, contributing to DNA demethylation and thus masking any molecular phenotype in *ssrp1-3* mutant pollen. Alternatively, the explanation may involve chromatin. Although vegetative and central cell nuclei are relatively decondensed (59), they have highly diverse fates: the vegetative cell undergoes no further division and is a terminally differentiated cell, whereas the central cell is fertilized and goes on to form the endosperm. It is likely the vegetative and central cells' chromatin

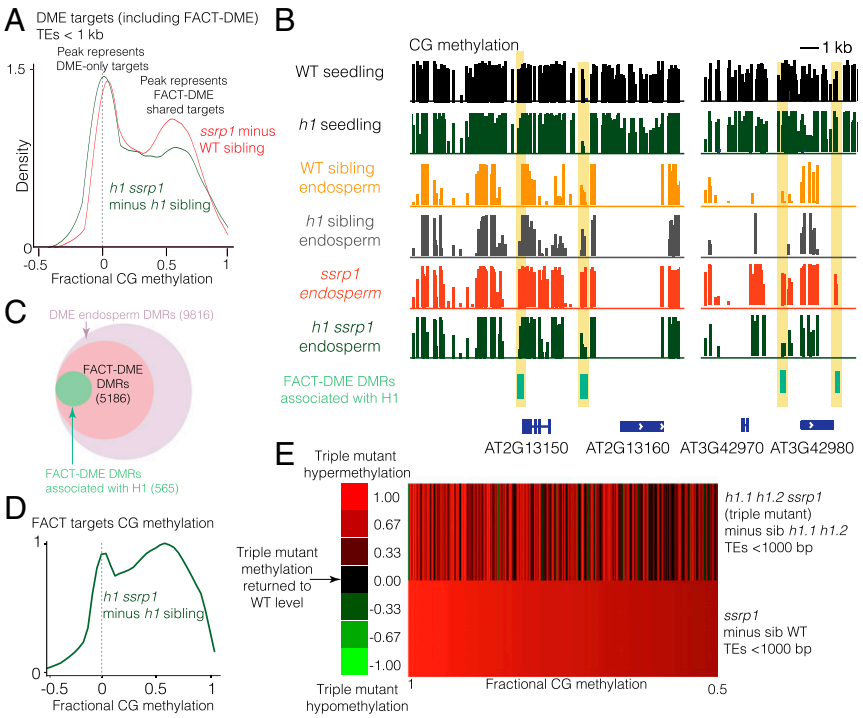

Fig. 7. H1 mediates the requirement for FACT at certain DME-target loci. (*A*) Kernel density plot of *h1.1/h1.2/ssrp1-3* (*h1 ssrp1*) triple-mutant endosperm (delayed) minus *h1.1/h1.2*/SSRP1 (*h1* sibling; normal development) endosperm maternal methylation compared with *ssrp1-3* (delayed) minus SSRP1 (WT sibling, normal development) maternal endosperm methylation, for DME targets only, in short TEs (<1 kb). (*B*) CG methylation profiles for WT and *h1* seedlings and for WT and *h1* sibling and *ssrp1* and *h1 ssrp1* mutant endosperm at examples of FACT-DME DMRs associated with H1. (*C*) Venn diagram to illustrate proportion of FACT-DME DMRs that are associated with H1 occupancy (565 DMRs, >20% methylation difference between *h1 ssrp1* and *ssrp1* mutant endosperm, $P < 0.001$). (*D*) Kernel density plot for the methylation status of *h1.1 h1.2 ssrp1* endosperm at FACT target sites only, showing two peaks. One peak is on zero and represents FACT target sites that are not hypermethylated in *h1.1 h1.2 ssrp1* (i.e., without H1); a lack of SSRP1 does not result in hypermethylation at these sites, likely since DME can access the chromatin at these sites without FACT. The second peak is at +0.5 fractional CG methylation and represents hypermethylated sites (i.e., those that still hypermethylated in the absence of H1), as DME still cannot access these loci without FACT. (*E*) Heat map detailing the methylation differences between *h1.1 h1.2 ssrp1* and *h1.1 h1.2* siblings compared with those between *ssrp1* and WT, at TEs <1,000 bp. Only FACT target sites are shown (i.e., hypermethylated from 0.5 to 1 fractional methylation difference in the *ssrp1* mutant compared with WT).

conformation will be different, which may explain why FACT is apparently not required for DME activity in pollen (60) but is needed in the central cell.

Experimental Procedures

See *SI Appendix, Supplementary Methods* for full methods. Sequencing data are deposited in the Gene Expression Omnibus database (accession no. GSE105000).

***Arabidopsis* Mutants.** The *ssrp1-3* (26) and *h1.1/h1.2* double mutants (49) were as described previously. The *spt16-3* T-DNA insertion line (GK_193H04) was obtained from the GABI-Kat collection (31) at the Nottingham Arabidopsis Stock Centre (61). All mutants were in the Col-0 background. T-DNA insertions were confirmed by PCR, and the location of *spt16-3* was identified using Sanger sequencing by the University of California, Berkeley DNA Sequencing Facility.

Isolation of *Arabidopsis* Endosperm and Embryos. WT Col-0 and mutant *Arabidopsis* flower buds were emasculated at flower stage 12 to 13 using fine forceps and pollinated with L*er* pollen 48 h later. Eight to 10 DAP, developing F1 seeds (torpedo to bending cotyledon stage) were immersed in dissection solution [filter-sterilized 0.3 M sorbitol and 5 mM (pH 5.7) MES] on sticky tape and dissected by hand under a stereomicroscope using fine forceps (Inox Dumont no. 5; Fine Science Tools) and insect mounting pins. The seed coat was discarded, and debris was removed by washing collected embryos or endosperm five to six times with dissection solution under the microscope. For *ssrp1-3* and *spt16-3* mutant normal and delayed sibling seed collection, seeds were divided into fractions according to embryo development. At 8 DAP, delayed seeds tended to be at the torpedo to early-linear cotyledon stages, whereas normally developing seeds were at the late-linear cotyledon to bending cotyledon stages (Figs. 1*B* and 3*B*). Seeds with an intermediate developmental stage were discarded.

Isolation of Vegetative Cell and Sperm Nuclei. Pollen was isolated from WT (Col-0) and *ssrp1-3* heterozygous plants as described previously (62, 63). Vegetative cell and sperm nuclei were extracted from mature pollen and fractionated by fluorescence-activated cell sorting as described previously (62, 63).

Bimolecular Fluorescence and Confocal Microscopy. To analyze the interaction between the DME protein and the FACT complex in vivo, full-length *cDME* (5.2 kb of the *At5g04560.2* transcript) was cloned into a *pSAT4-nEYFP-C1* vector. Both C-terminal *cSPT16* (1.9 kb) and N-terminal *cSSRP1* (1.9 kb) were cloned into a *pSAT4-cEYFP-C1-B* vector. Pairs of constructs were introduced into *Arabidopsis* leaf protoplasts by PEG transfection as described previously (64). After incubation, fluorescence was observed using the Zeiss Confocal Laser Scanning Microscope LSM700.

ACKNOWLEDGMENTS. We thank Christina Wistrom for her management of the University of California, Berkeley, Oxford Tract greenhouse facility. We are grateful to Jessica Rodrigues, Tzung-Fu Hsieh, and David Lyons for helpful discussions on this work. This work used the Vincent J. Coates Genomics Sequencing Laboratory at the University of California, Berkeley, supported by NIH S10 Instrumentation Grants S10RR029668, S10RR027303, and S10OD018174, and the authors would like to particularly thank Shana McDevitt for her assistance. This work was funded by the NSF Grant IOS-1025890 and the NIH Grant R01-GM069415 (to D.Z. and R.L.F.), by the National Research Foundation of Korea Grant 2017R1A2B2007067 and the Next-Generation BioGreen 21 Program Grant PJ013127 (to Y.C.), and by the Grants-in-Aid for Scientific Research (KAKENHI) Grant JP16H06471 (to T.K.).

1. Law JA, Jacobsen SE (2010) Establishing, maintaining and modifying DNA methylation patterns in plants and animals. *Nat Rev Genet* 11:204–220.
2. Du J, Johnson LM, Jacobsen SE, Patel DJ (2015) DNA methylation pathways and their crosstalk with histone methylation. *Nat Rev Mol Cell Biol* 16:519–532.
3. Roudier F, Teixeira FK, Colot V (2009) Chromatin indexing in *Arabidopsis*: An epigenomic tale of tails and more. *Trends Genet* 25:511–517.
4. Kim MY, Zilberman D (2014) DNA methylation as a system of plant genomic immunity. *Trends Plant Sci* 19:320–326.
5. Bewick AJ, Schmitz RJ (2017) Gene body DNA methylation in plants. *Curr Opin Plant Biol* 36:103–110.
6. Gehring M, Reik W, Henikoff S (2009) DNA demethylation by DNA repair. *Trends Genet* 25:82–90.
7. Monk M, Boubelik M, Lehnert S (1987) Temporal and regional changes in DNA methylation in the embryonic, extraembryonic and germ cell lineages during mouse embryo development. *Development* 99:371–382.
8. Feng S, Jacobsen SE, Reik W (2010) Epigenetic reprogramming in plant and animal development. *Science* 330:622–627.
9. Ibarra CA, et al. (2012) Active DNA demethylation in plant companion cells reinforces transposon methylation in gametes. *Science* 337:1360–1364.
10. Park K, et al. (2016) DNA demethylation is initiated in the central cells of *Arabidopsis* and rice. *Proc Natl Acad Sci USA* 113:15138–15143.
11. Park J-S, et al. (2017) Control of DEMETER DNA demethylase gene transcription in male and female gamete companion cells in *Arabidopsis thaliana*. *Proc Natl Acad Sci USA* 114:2078–2083.
12. Satyaki PRV, Gehring M (2017) DNA methylation and imprinting in plants: Machinery and mechanisms. *Crit Rev Biochem Mol Biol* 52:163–175.
13. Kinoshita T, Yadegari R, Harada JJ, Goldberg RB, Fischer RL (1999) Imprinting of the MEDEA polycomb gene in the *Arabidopsis* endosperm. *Plant Cell* 11:1945–1952.
14. Köhler C, Makarevich G (2006) Epigenetic mechanisms governing seed development in plants. *EMBO Rep* 7:1223–1227.
15. Hehenberger E, Kradolfer D, Köhler C (2012) Endosperm cellularization defines an important developmental transition for embryo development. *Development* 139: 2031–2039.
16. Choi Y, et al. (2002) DEMETER, a DNA glycosylase domain protein, is required for endosperm gene imprinting and seed viability in arabidopsis. *Cell* 110:33–42.
17. Gehring M, et al. (2006) DEMETER DNA glycosylase establishes MEDEA polycomb gene self-imprinting by allele-specific demethylation. *Cell* 124:495–506.
18. Hsieh T-F, et al. (2009) Genome-wide demethylation of *Arabidopsis* endosperm. *Science* 324:1451–1454.
19. Tessarz P, Kouzarides T (2014) Histone core modifications regulating nucleosome structure and dynamics. *Nat Rev Mol Cell Biol* 15:703–708.
20. Belotserkovskaya R, et al. (2003) FACT facilitates transcription-dependent nucleosome alteration. *Science* 301:1090–1093.
21. Formosa T (2012) The role of FACT in making and breaking nucleosomes. *Biochim Biophys Acta* 1819:247–255.
22. Heo K, et al. (2008) FACT-mediated exchange of histone variant H2AX regulated by phosphorylation of H2AX and ADP-ribosylation of Spt16. *Mol Cell* 30:86–97.
23. Orphanides G, Wu WH, Lane WS, Hampsey M, Reinberg D (1999) The chromatin-specific transcription elongation factor FACT comprises human SPT16 and SSRP1 proteins. *Nature* 400:284–288.
24. Okuhara K, et al. (1999) A DNA unwinding factor involved in DNA replication in cell-free extracts of Xenopus eggs. *Curr Biol* 9:341–350.
25. Duroux M, Houben A, Rúzicka K, Friml J, Grasser KD (2004) The chromatin remodelling complex FACT associates with actively transcribed regions of the *Arabidopsis* genome. *Plant J* 40:660–671.
26. Ikeda Y, et al. (2011) HMG domain containing SSRP1 is required for DNA demethylation and genomic imprinting in *Arabidopsis*. *Dev Cell* 21:589–596.
27. Lolas IB, et al. (2010) The transcript elongation factor FACT affects *Arabidopsis* vegetative and reproductive development and genetically interacts with HUB1/2. *Plant J* 61:686–697.
28. Winkler DD, Luger K (2011) The histone chaperone FACT: Structural insights and mechanisms for nucleosome reorganization. *J Biol Chem* 286:18369–18374.
29. Bauer MJ, Fischer RL (2011) Genome demethylation and imprinting in the endosperm. *Curr Opin Plant Biol* 14:162–167.
30. Jullien PE, Susaki D, Yelagandula R, Higashiyama T, Berger F (2012) DNA methylation dynamics during sexual reproduction in *Arabidopsis thaliana*. *Curr Biol* 22:1825–1830.
31. Kleinboelting N, Huep G, Kloetgen A, Viehoever P, Weisshaar B (2012) GABI-Kat SimpleSearch: ew features of the *Arabidopsis thaliana* T-DNA mutant database. *Nucleic Acids Res* 40:D1211–D1215.
32. Kodama Y, Hu C-D (2012) Bimolecular fluorescence complementation (BiFC): A 5-year update and future perspectives. *Biotechniques* 53:285–298.
33. Jeong CW, et al. (2015) Control of paternally expressed imprinted UPWARD CURLY LEAF1, a gene encoding an F-box protein that regulates CURLY leaf polycomb protein, in the *Arabidopsis* endosperm. *PLoS One* 10:e0117431.
34. Hsieh T-F, et al. (2011) Regulation of imprinted gene expression in *Arabidopsis* endosperm. *Proc Natl Acad Sci USA* 108:1755–1762.
35. Schon MA, Nodine MD (2017) Widespread contamination of arabidopsis embryo and endosperm transcriptome data sets. *Plant Cell* 29:608–617.
36. Chaudhury AM, et al. (1997) Fertilization-independent seed development in *Arabidopsis thaliana*. *Proc Natl Acad Sci USA* 94:4223–4228.
37. Qian W, et al. (2012) A histone acetyltransferase regulates active DNA demethylation in *Arabidopsis*. *Science* 336:1445–1448.
38. Qian W, et al. (2014) Regulation of active DNA demethylation by an α-crystallin domain protein in *Arabidopsis*. *Mol Cell* 55:361–371.
39. Sequeira-Mendes J, et al. (2014) The functional topography of the *Arabidopsis* genome is organized in a reduced number of linear motifs of chromatin states. *Plant Cell* 26:2351–2366.
40. Chodavarapu RK, et al. (2010) Relationship between nucleosome positioning and DNA methylation. *Nature* 466:388–392.
41. Bernatavichute YV, Zhang X, Cokus S, Pellegrini M, Jacobsen SE (2008) Genome-wide association of histone H3 lysine nine methylation with CHG DNA methylation in *Arabidopsis thaliana*. *PLoS One* 3:e3156.
42. Kim SY, Lee J, Eshed-Williams L, Zilberman D, Sung ZR (2012) EMF1 and PRC2 cooperate to repress key regulators of *Arabidopsis* development. *PLoS Genet* 8: e1002512.
43. Yelagandula R, et al. (2014) The histone variant H2A.W defines heterochromatin and promotes chromatin condensation in *Arabidopsis*. *Cell* 158:98–109.
44. Roudier F, et al. (2011) Integrative epigenomic mapping defines four main chromatin states in *Arabidopsis*. *EMBO J* 30:1928–1938.
45. Jacob Y, et al. (2009) ATXR5 and ATXR6 are H3K27 monomethyltransferases required for chromatin structure and gene silencing. *Nat Struct Mol Biol* 16:763–768.
46. Postnikov YV, Bustin M (2016) Functional interplay between histone H1 and HMG proteins in chromatin. *Biochim Biophys Acta* 1859:462–467.
47. Raghuram N, Carrero G, Th'ng J, Hendzel MJ (2009) Molecular dynamics of histone H1. *Biochem Cell Biol* 87:189–206.
48. Harshman SW, Young NL, Parthun MR, Freitas MA (2013) H1 histones: Current perspectives and challenges. *Nucleic Acids Res* 41:9593–9609.
49. Zemach A, et al. (2013) The *Arabidopsis* nucleosome remodeler DDM1 allows DNA methyltransferases to access H1-containing heterochromatin. *Cell* 153:193–205.
50. Xin H, et al. (2009) yFACT induces global accessibility of nucleosomal DNA without H2A-H2B displacement. *Mol Cell* 35:365–376.
51. Böhm V, et al. (2011) Nucleosome accessibility governed by the dimer/tetramer interface. *Nucleic Acids Res* 39:3093–3102.
52. Pavri R, et al. (2006) Histone H2B monoubiquitination functions cooperatively with FACT to regulate elongation by RNA polymerase II. *Cell* 125:703–717.
53. Biswas D, et al. (2006) Opposing roles for Set2 and yFACT in regulating TBP binding at promoters. *EMBO J* 25:4479–4489.
54. Fleming AB, Kao C-F, Hillyer C, Pikaart M, Osley MA (2008) H2B ubiquitylation plays a role in nucleosome dynamics during transcription elongation. *Mol Cell* 31:57–66.
55. Charles Richard JL, et al. (2016) FACT assists base excision repair by boosting the remodeling activity of RSC. *PLoS Genet* 12:e1006221.
56. Kalashnikova AA, et al. (2013) Linker histone H1.0 interacts with an extensive network of proteins found in the nucleolus. *Nucleic Acids Res* 41:4026–4035.
57. Szerlong HJ, et al. (2015) Proteomic characterization of the nucleolar linker histone H1 interaction network. *J Mol Biol* 427:2056–2071.
58. Catez F, Hock R (2010) Binding and interplay of HMG proteins on chromatin: Lessons from live cell imaging. *Biochim Biophys Acta* 1799:15–27.
59. Gutierrez-Marcos JF, Dickinson HG (2012) Epigenetic reprogramming in plant reproductive lineages. *Plant Cell Physiol* 53:817–823.
60. Slotkin RK, et al. (2009) Epigenetic reprogramming and small RNA silencing of transposable elements in pollen. *Cell* 136:461–472.
61. Scholl RL, May ST, Ware DH (2000) Seed and molecular resources for *Arabidopsis*. *Plant Physiol* 124:1477–1480.
62. Schoft VK, et al. (2009) Induction of RNA-directed DNA methylation upon decondensation of constitutive heterochromatin. *EMBO Rep* 10:1015–1021.
63. Schoft VK, et al. (2011) Function of the DEMETER DNA glycosylase in the *Arabidopsis thaliana* male gametophyte. *Proc Natl Acad Sci USA* 108:8042–8047.
64. Yoo S-D, Cho Y-H, Sheen J (2007) *Arabidopsis* mesophyll protoplasts: A versatile cell system for transient gene expression analysis. *Nat Protoc* 2:1565–1572.